\



Separating spins by dwell time of electrons across parallel double δ-magnetic-barrier nanostructure applied by bias

Sai-Yan Chen(陈赛艳), Mao-Wang Lu(卢卯旺), and Xue-Li Cao(曹雪丽)

Citation: Chin. Phys. B, 2022, 31 (**1**): 017201. DOI: 10.1088/1674-1056/abeb09
Journal homepage: http://cpb.iphy.ac.cn; http://iopscience.iop.org/cpb

What follows is a list of articles you may be interested in

Evaluation of stress voltage on off-state time-dependent breakdown for GaN MIS-HEMT with SiN_x gate dielectric

Tao-Tao Que(阙陶陶), Ya-Wen Zhao(赵亚文), Qiu-Ling Qiu(丘秋凌), Liu-An Li(李柳暗), Liang He(何亮), Jin-Wei Zhang(张津玮), Chen-Liang Feng(冯辰亮), Zhen-Xing Liu(刘振兴), Qian-Shu Wu(吴千树), Jia Chen(陈佳), Cheng-Lang Li(黎城朗), Qi Zhang(张琦), Yun-Liang Rao(饶运良), Zhi-Yuan He(贺致远), and Yang Liu (刘扬)†
Chin. Phys. B, 2020, 29 (**10**): 107201. DOI: 10.1088/1674-1056/abaed8

Experimental evaluation of interface states during time-dependent dielectric breakdown of GaN-based MIS-HEMTs with LPCVD-SiN_x gate dielectric

Ya-Wen Zhao(赵亚文), Liu-An Li(李柳暗), Tao-Tao Que(阙陶陶), Qiu-Ling Qiu(丘秋凌), Liang He(何亮), Zhen-Xing Liu(刘振兴), Jin-Wei Zhang(张津玮), Qian-Shu Wu(吴千树), Jia Chen(陈佳), Zhi-Sheng Wu(吴志盛), Yang Liu(刘扬)
Chin. Phys. B, 2020, 29 (**6**): 067203. DOI: 10.1088/1674-1056/ab8895

Effect of overdrive voltage on PBTI trapping behavior in GaN MIS-HEMT with LPCVD SiN_x gate dielectric

Tao-Tao Que(阙陶陶), Ya-Wen Zhao(赵亚文), Liu-An Li(李柳暗), Liang He(何亮), Qiu-Ling Qiu(丘秋凌), Zhen-Xing Liu(刘振兴), Jin-Wei Zhang(张津玮), Jia Chen(陈佳), Zhi-Sheng Wu(吴志盛), Yang Liu(刘扬)
Chin. Phys. B, 2020, 29 (**3**): 037201. DOI: 10.1088/1674-1056/ab696b

Effects of interface bound states on the shot noise in normal metal-low-dimensional Rashba semiconductor tunnel junctions with induced s-wave pairing potential

Wen-Xiang Chen(陈文祥), Rui-Qiang Wang(王瑞强), Liang-Bin Hu(胡梁宾)
Chin. Phys. B, 2019, 28 (**5**): 057201. DOI: 10.1088/1674-1056/28/5/057201

Magnetization-direction-dependent inverse spin Hall effect observed in IrMn/NiFe/Cu/YIG multilayer structure

Runrun Hao(郝润润), Ruxue Zang(臧如雪), Tie Zhou(周铁), Shishou Kang(康仕寿), Shishen Yan(颜世申), Guolei Liu(刘国磊), Guangbing Han(韩广兵), Shuyun Yu(于淑云), Liangmo Mei(梅良模)
Chin. Phys. B, 2019, 28 (**3**): 037202. DOI: 10.1088/1674-1056/28/3/037202

Separating spins by dwell time of electrons across parallel double δ-magnetic-barrier nanostructure applied by bias

Sai-Yan Chen(陈赛艳)†, Mao-Wang Lu(卢卯旺), and Xue-Li Cao(曹雪丽)

College of Science, Guilin University of Technology, Guilin 541004, *China*

(Received 17 January 2021; revised manuscript received 18 February 2021; accepted manuscript online 2 March 2021)

The dwell time and spin polarization (SP) of electrons tunneling through a parallel double δ-magnetic-barrier nanostructure in the presence of a bias voltage is studied theoretically in this work. This nanostructure can be constructed by patterning two asymmetric ferromagnetic stripes on the top and bottom of InAs/$Al_xIn_{1-x}As$ heterostructure, respectively. An evident SP effect remains after a bias voltage is applied to the nanostructure. Moreover, both magnitude and sign of spin-polarized dwell time can be manipulated by properly changing the bias voltage, which may result in an electrically-tunable temporal spin splitter for spintronics device applications.

Keywords: parallel double δ-magnetic-barrier nanostructure, bias, dwell time, spin polarization, temporal spin splitter

PACS: 72.25.Dc, 72.25.–b, 72.25.Hg, 85.75.–d **DOI:** 10.1088/1674-1056/abeb09

1. Introduction

With the development of modern material growth technology, nano-scaled magnetic materials can now be deposited on the surfaces of semiconductor heterostructures experimentally.[1] The movement of high-mobility two-dimensional electron gas (2DEG) embedded in the interface of semiconductor heterostructure can be controlled by an inhomogeneous magnetic field. Such a semiconductor heterostructure includes the so-called magnetic modulation semiconductor nanostructures (MMSN),[2] such as magnetic barriers (MB), magnetic traps, and magnetic superlattices. The MMSN is a small quantum system composed of semiconductor and magnetic materials. Beside the advantages of small size, low dimensionality, and local magnetic confinement, the MMSN has abundant physical properties, such as magnetic edge states,[3] wave-vector filtering,[4] magnetoresistance resonance,[5] giant magnetoresistance (GMR),[6,7] and spin polarization (SP).[8,9] These physical properties can be used to design new types of nanoelectronics devices, such as spin filters,[10] GMR devices,[11] momentum filters,[12] and spatial spin filters.[13] Therefore, the study of electron-spin transport characteristics in MMSN has attracted the great research interest.[14–20]

Two methods are used to study the electron-spin transport properties in MMSNs. The first method is to use the spin filtering of an MMSN, which gives rise to the electron-spin filter. When electron tunneling through the MMSN, the electron spin in a certain direction is suppressed, and the SP of electrons in semiconductor is realized.[21–25] The second method used to realize SP is to use the Goos–Hänchen (GH) effect for electron beam in MMSN, *i.e.*, spatially separating electron spins by GH displacement when electron beam traverses an MMSN, that is, the semiconductor nanostructure is devised as a spatial spin filter.[26–30] Meanwhile, another method is used specifically for separating electron spins in time dimension. This method of separating electron spins is to utilize different transmission times of electrons tunneling through the MMSN. The transmission time can help understand the dynamic response process of electronic device. Importantly, we can find a new way to realize the SP, that is, to separate electron spins in time dimension for injecting spin-polarized electrons into semiconductor. In 2002, Zhai *et al.*[31] took the square MB MMSN for example and studied the transmission time of electrons in the MMSN. They used the group velocity method to calculate the group delay time of electrons. One year later, Xu *et al.*[32] calculated the phase delay time in δ-MB MMSN by using the stationary phase method, and put forward the idea of using the transmission time of electrons to separate spins in time dimension. However, in quantum mechanics, time is not an operator. Therefore, the measurement of time is still controversial in academia. Thus far, at least seven different definitions have been proposed to describe time, two of which, the dwell time and the group delay time, are widely accepted.[33] In 2003, Winful[34] discovered the relationship among these times, that is, $t_{\rm dwell} = t_{\rm group} - t_{\rm inter}$ where $t_{\rm inter}$ is the self-interference delay time between incident wave and reflection wave, and thus unified the transmission time calculation into the dwell time.[35]

Very recently, Lu *et al.*[36,37] and Guo *et al.*[38] investigated the transmission time and the spin polarization of electrons tunneling through an MMSN. They observed that dwell time is spin-related, and the magnitude and sign of spin-polarized dwell time can be adjusted by changing δ-doping or an applied voltage. In this paper, applying a bias voltage to a parallel double δ-MB nanostructure, we investigate the dwell

†Corresponding author. E-mail: 6615049@glut.edu.cn

© 2022 Chinese Physical Society and IOP Publishing Ltd

time and the SP of electrons in accordance with Winful's theory, and focus on the separation and control of electron spins in time dimension.

2. Theory and method

We consider a parallel double δ-MB nanostructure as described in Fig. 1(a), which can be fabricated by patterning two asymmetric FM stripes on the top and bottom of InAs/$Al_xIn_{1-x}As$ heterostructure, respectively. The structural model is shown in Fig. 1(b), where a bias voltage V_α is applied to the MMSN along the electronic transport direction. The magnetic field excited by the FM stripe can be expressed as $\boldsymbol{B} = B_z(x)\hat{e}_z$ with $B_z(x) = B[\delta(x) + \delta(x-L)]$, where B is the magnetic strength of δ-MBs. A negative voltage is applied to the upper FM stripe, and the electric-barrier (EB) induced by this applied voltage is viewed to be rectangular, and expressed as $U(x) = U[\Theta(L-x) - \Theta(x)]$, where U is the EB height. Under the Landau gauge, the magnetic vector potential can be given by $\boldsymbol{A}(x) = [0, A_y(x), 0]$ with

$$A_y(x) = \begin{cases} 0, & x < 0, \\ B, & 0 < x < L, \\ 2B, & x > L. \end{cases} \tag{1}$$

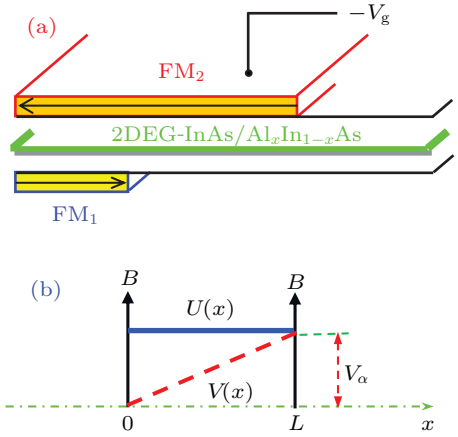


Fig. 1. (a) Schematic diagram of MMSN and (b) magnetic profile and bias voltage.

Assuming that $B_z(x)$ and $U(x)$ are constant on the y axis and change only on the x axis, the Hamiltonian describing electrons in such an MMSN in the presence of a bias can be given, in a single particle, effective mass approximation, as follows:

$$H = \frac{p_x^2}{2m^*} + \frac{[p_y + eA_y(x)]^2}{2m^*} + U(x) + \frac{1}{2}g^*\mu_B\sigma_z B_z(x) + \frac{eV_\alpha x}{L}, \tag{2}$$

where m^*, $\boldsymbol{p}$, e, m_0, and g^* are the effective mass, momentum, charge, free mass, and effective g-factor of an electron, respectively, $\mu_B = e\hbar/2m_0$ is the Bohr magneton, and $\sigma_z = +1/-1$ represents spin-up/down electron. For convenience, all physical quantities are expressed in dimensionless forms, *e.g.*, $B_z(x) \to B_0 B_z(x)$, $A(x) \to B_0 \ell_{B_0} A(x)$, $x \to \ell_{B_0} x$, $k \to k/\ell_{B_0}$, $E \to \hbar\omega_c E = E_0 E$, $V_\alpha(x) \to V_\alpha(x) E_0/e$, and $t \to t\tau_0$, where $\ell_{B_0} = \sqrt{\hbar/eB_0}$, $E_0 = \hbar eB_0/m^*$, and $\tau_0 = m^*/eB_0$.

For an MMSN, the motion of an electron in the y direction is conserved, therefore, its wave function can be written as $\Phi(x,y) = e^{ik_y y}\psi(x)$, where k_y is the y component of the wave vector. The wave function, $\psi(x)$, satisfies the reduced one-dimensional Schrödinger equation

$$\left\{\frac{d^2}{dx^2} + 2[E - U_{\text{eff}}(x, k_y, \sigma_z, U, V_\alpha)]\right\}\psi(x) = 0, \tag{3}$$

where the effective potential experienced by electrons in this parallel double δ-MB nanostructure can be written as follows:

$$U_{\text{eff}}(x, k_y, \sigma_z, U, V_\alpha) = \frac{1}{2}[A_y(x) + k_y]^2 + U(x) + \frac{m^* g^* \sigma_z B_z(x)}{4m_0} + \frac{eV_\alpha}{L}x. \tag{4}$$

Evidently, this effective potential is related to not only the magnetic field $B_z(x)$, wave vector k_y, and EB $U(x)$, but also the bias voltage V_α. It is difficult to exactly solve Eq. (3) due to the complicated effective potential. Here, we use improved transfer-matrix method (ITMM)[12] to numerically solve Eq. (3). The wave functions of electron can be expressed, in linear combination of plane waves, by

$$\begin{cases} \psi_{\text{left}}(x) = e^{ik_l x} + \gamma e^{-ik_l x}, & x < 0, \\ \psi_{\text{int}}(x) = Ce^{ikx} + De^{-ikx}, & 0 < x < L, \\ \psi_{\text{right}}(x) = \tau e^{ik_r x}, & x > L, \end{cases} \tag{5}$$

where $k_\ell = \sqrt{2E - k_y^2}$, $k = \sqrt{2(E-U) - (k_y + B)^2 - 2V_\alpha x/L}$, and $k_r = \sqrt{2(E - V_\alpha) - (k_y + 2B)^2}$, γ/τ is the reflection/transmission amplitude, and C/D is the pending constant. In accordance with the continuity condition of these wave functions at the boundaries, we can obtain

$$\begin{pmatrix} e^{ik_l x_0} & e^{-ik_l x_0} \\ (2V_1 + ik_l)e^{ik_l x_0} & (2V_1 - ik_l)e^{-ik_l x_0} \end{pmatrix}\begin{pmatrix} 1 \\ \gamma \end{pmatrix} = M\begin{pmatrix} e^{ik_r x_L} & e^{-ik_r x_L} \\ (ik_r - 2V_1)e^{ik_r x_L} & (-ik_r - 2V_1)e^{-ik_l x_0} \end{pmatrix}\begin{pmatrix} \tau \\ 0 \end{pmatrix}, \tag{6}$$

where $M = \begin{pmatrix} M_{11} & M_{12} \\ M_{21} & M_{22} \end{pmatrix}$ is the total transfer matrix, and $V_1 = 0.09B\sigma_z$. Solving Eq. (6), we can obtain the amplitude of the transmitted wave and reflected wave as follows:

$$\tau(E, k_y, \sigma_z, U, V_\alpha) = \frac{2ik_l}{[(M_{21} - 2V_1(M_{11} + M_{22}) + (4V_1^2 - k_r k_l)M_{12}] + i[k_r M_{22} + k_l M_{11} - 2V_1 M_{12}(k_r + k_l)]}, \tag{7}$$

$$\gamma(E,k_y,U,V_\alpha)=\frac{\left[(M_{21}-2V_1(M_{11}+M_{22})+\left(4V_1^2+k_rk_l\right)M_{12}\right]+\mathrm{i}\left[k_rM_{22}-k_lM_{11}+2V_1M_{12}(k_l-k_r)\right]}{\left[(-M_{21}+2V_1(M_{11}+M_{22})+\left(k_rk_l-4V_1^2\right)M_{12}\right]+\mathrm{i}\left[-k_rM_{22}-k_lM_{11}+2V_1M_{12}(k_r+k_l)\right]}. \tag{8}$$

Thus, we can calculate the group delay time and the self-interference delay time of electron tunneling through this parallel double δ-MB nanostructure, respectively,

$$\begin{aligned} &t_g^{\sigma_z}(E,k_y,U,\sigma_z,V_\alpha)\\ &=|\tau|^2\times\frac{\partial}{\partial E}\left[\arg(\tau)\right]+|\gamma|^2\times\frac{\partial}{\partial E}\left[\arg(\gamma)\right], \end{aligned} \tag{9}$$

$$t_i^{\sigma_z}(E,k_y,U,\sigma_z,V_\alpha)=-\frac{\mathrm{Im}(\gamma)}{k_l}\times\frac{\partial k_l}{\partial E}. \tag{10}$$

Following Winful's theory,[34] the dwell time for electrons across this MMSN can be obtained from

$$\begin{aligned} &\tau_d^{\sigma_z}(E,k_y,U,\sigma_z,V_\alpha)\\ &=\tau_g^{\sigma_z}(E,k_y,U,V_\alpha,x_0)-\tau_i^{\sigma_z}(E,k_y,U,V_\alpha,x_0). \end{aligned} \tag{11}$$

Using the dwell time, spin polarization of dwell time SP can be characterized by

$$P_t=\frac{t_d^{\uparrow}(E,k_y,U,\sigma_z,V_\alpha)-t_d^{\downarrow}(E,k_y,U,\sigma_z,V_\alpha)}{t_d^{\uparrow}(E,k_y,U,V_\alpha)+t_d^{\downarrow}(E,k_y,U,V_\alpha)}, \tag{12}$$

where $t_d^{\uparrow}(E,k_y,U,V_\alpha)$ and $t_d^{\downarrow}(E,k_y,U,V_\alpha)$ denote the dwell time of spin-up and spin-down electrons, respectively.

Here, because time is not an operator in quantum mechanics, how to measure the tunneling time is a controversial problem. So far, the measuring of time is defined in different ways, *e.g.*, the dwell time and the group delay. In this paper, we adopt the dwell time through using plane waves (not wave packets). The temporal separation of the electron spins is usually on the order of 10 ps, which is faster than current operation speed in nanoelectronics and must require advanced techniques to be measured. In our model, the relaxation process is not involved, which deserves to be explored in the future.

3. Results and discussion

In our numerical calculation, the InAs system ($g^*=15$ and $m^*_{\mathrm{InAs}}=0.024m_0$) is considered as two-dimensional electron gas (2DEG) material, which possesses the basic parameters $\ell_{\mathrm{B}}=81.3$ nm, $E_0=0.48$ meV, and $\tau_0=1.39$ ps for a typical magnetic field $B_0=0.1T$.[8] Thereafter, the partial structural parameters are set to be $B=2.0$, $k_y=0.7$, and $U=9.0$, unless otherwise stated. Figure 2(a) shows the dwell time of electrons tunneling through this parallel double δ-MB nanostructure, where solid and dashed lines correspond to spin-up and spin-down electrons, respectively. The difference in dwell time between spin-up and spin-down electrons can be observed. Thus, this MMSN still exhibits a significant SP effect when a bias voltage is applied. This phenomenon stems from the spin–field interaction between the electron spin and structural magnetic field. In addition, a peak appears in the dwell time spectrum, that is, the dwell time achieves a maximal value at resonance, where the incident energy of electrons is equal to the binding energy in the MMSN. This spin-dependent dwell time of electrons tunneling through this MMSN indicates that electron spins can be separated in the time dimension, and this finding may be useful for spintronics device applications. Figure 2(b) presents the SP of dwell time as a function of incident energy, where the green and red curves denote the bias voltages $V_\alpha=0.0$, and $V_\alpha=2.0$, respectively. This figure shows that an evident SP effect in dwell time occurs when electrons tunnel through this nanostructure. Moreover, when a bias voltage is applied to this MMSN, the SP effect of electrons is enhanced, and the SP curve shifts toward the high-energy region.

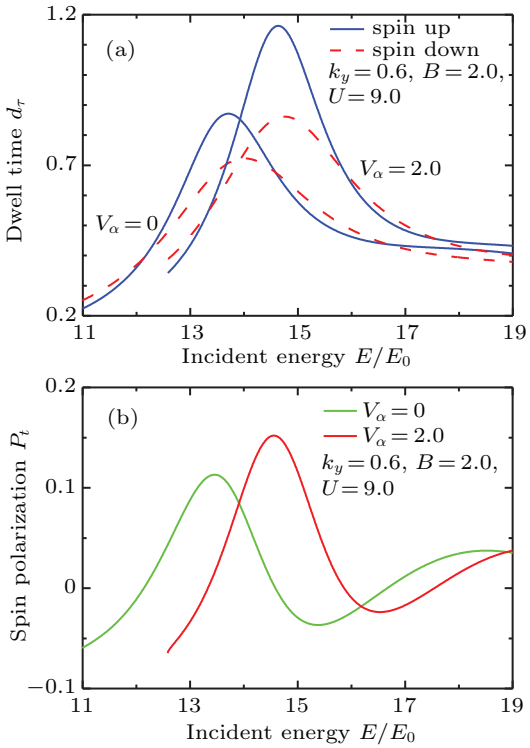


Fig. 2. Curves of (a) dwell time and (b) spin polarization of electron *versus* incident energy for different parameters.

A controllable spin-polarized source is desired for spintronics device applications.[39] Having known a considerable SP effect in this parallel double δ-MB nanostructure when a bias voltage is applied, we next study how such a bias affects the spin-polarized dwell time. First, we apply a positive bias to this parallel double δ-MB nanostructure and investigate the effect of positive bias on the spin-polarized dwell time. Figure 3(a) shows the variations of spin-polarized dwell time with incident energy for three bias voltages: $V_\alpha=0.0$ (green curve), 2.0 (red curve), and 3.0 (blue curve). Evidently, the SP ratio

of dwell time is closely related to the positive bias voltage. When a positive bias is applied to this nanostructure, the spin-polarized dwell time increases, and the SP curve of dwell time shifts slightly toward the high-energy region. The figure also shows that the SP ratio of dwell time is related to the incident energy. To further observe the influence of bias voltage on the SP ratio of dwell time, in Fig. 4(b) we directly draw the curves of the spin-polarized dwell time *versus* bias voltage for three fixed values of incident energy $E = 14.0$ (green curve), 15.0 (red curve), and 16.0 (blue curve). Both magnitude and sign of spin-polarized dwell time greatly change with bias voltage. Moreover, the peak of SP ratio of dwell time increases with bias voltage increasing, and the SP curve shifts rightwards. Clearly, the effect of bias voltage on spin-polarized dwell time results from the dependence of $U_{\text{eff}}(E, k_y, \sigma_z, V_\alpha, x_0)$ on V_α. This phenomenon implies that we can control the spin-polarized dwell time by adjusting the bias voltage.

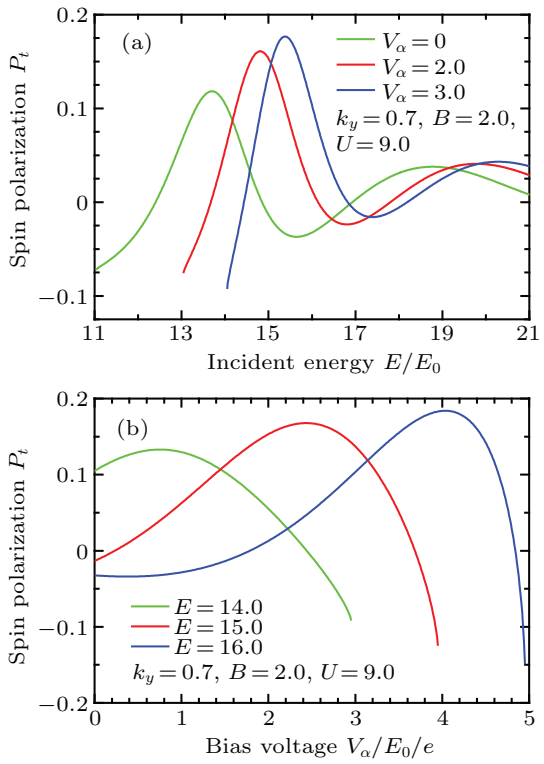


Fig. 3. Curves of spin polarization *versus* (a) incident energy and (b) bias voltage for different parameters.

Next, we investigate the effect of a negative bias voltage on the spin-polarized dwell time. Figure 4(a) shows the relation between spin-polarized dwell time and the incident energy, where the bias voltage values are fixed at $V_\alpha = 0.0$ (green curve) -2.0 (red curve), and -3.0 (blue curve), respectively, and the structural parameters are exactly the same as those in Fig. 3(a). Evidently, the negative bias voltage also affects the SP of dwell time. However, with the increase of the applied negative bias voltage, the SP of dwell time gradually is weakened, and the SP curve shifts toward the low-energy region. Figure 4(b) shows the influence of negative bias voltage on spin-polarized dwell time. The figure indicates the change of SP of dwell time with negative bias voltage, where the incident energy values are set to be $E = 14.0$ (green curve), 15.0 (red curve), and 16.0 (blue curve), respectively. Figure 4(b) also confirms that the SP ratio of dwell time changes drastically with negative bias voltage. In addition, when the incident energy changes, the SP ratio varies correspondingly. Therefore, spin-polarized dwell time in this parallel double δ-MB nanostructure can be controlled by adjusting the negative bias voltage.

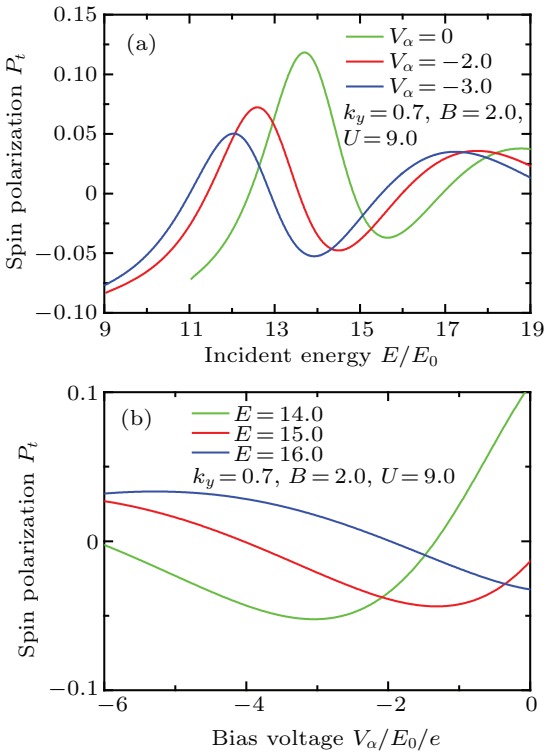


Fig. 4. Curves of spin polarization *versus* (a) incident energy and (b) bias voltage for different parameters.

4. Conclusions

In this work, we investigate the dwell time and the SP of electrons tunneling through a parallel double δ-MB nanostructure with a bias voltage, which is constructed by patterning two asymmetric FM stripes on the top and bottom of InAs/Al$_x$In$_{1-x}$As heterostructure, respectively. It is shown that this MMSN still possesses an appreciable SP effect despite a bias voltage is presented inside, which is due to the spin–field interaction between the electron spin and structural magnetic field. It is also shown that both amplitude and sign of the SP can be controlled by appropriately changing the bias voltage, which may lead to an electrically-controllable temporal spin splitter for spintronic device applications.

Acknowledgement

Project supported by the National Natural Science Foundation of China (Grant No. 11864009).

References

[1] Kubrak V, Rahman F, Gallagher B L, Main P C, Henini M, Marrows C H and Howson M A 1999 *Appl. Phys. Lett.* **74** 2507

[2] Matulis A, Peeters F M and Vasilopoulos P 1994 *Phys. Rev. Lett.* **72** 1518

[3] Sim H S, Ahn K H and Chang K J 1998 *Phys. Rev. Lett.* **80** 1501

[4] Kong Y H, Lu K Y, He Y P, Liu X H, Fu X and Li A H 2018 *Appl. Phys. A* **124** 440

[5] Nogaret A, Bending S J and Henini M 2000 *Phys. Rev. Lett.* **84** 2231

[6] Zhai F, Guo Y and Gu B L 2002 *Phys. Rev. B* **66** 125305

[7] Jiang Y Q, Lu M W, Huang X H, Yang S P and Tang Q 2016 *J. Electron. Mater.* **45** 2796

[8] Papp G and Peeters F M 2001 *Appl. Phys. Lett.* **78** 2184

[9] Yang S P, Lu M W, Huang X H, Tang Q and Zhou Y L 2017 *J. Electron. Mater.* **46** 1937

[10] Lu M W, Chen S Y, Zhang G L and Huang X H 2018 *IEEE Trans. Electron. Dev.* **65** 3045

[11] Lu M W, Cao X L, Huang X H, Jiang Y Q and Yang S P 2018 *Appl. Surf. Sci.* **360** 989

[12] Lu M W, Chen S Y and Zhang G L 2017 *IEEE Trans. Electron. Dev.* **64** 1825

[13] Lu M W, Cao X L, Huang X H, Jiang Y Q and Li S 2014 *J. Appl. Phys.* **115** 174305

[14] Guo Y, Gu B L, Zeng Z and Yu J Z and Kawazoe Y 2000 *Phys. Rev. B* **62** 2635

[15] Wu W and Xu H Q 2006 *Appl. Phys. Lett.* **88** 032502

[16] Zhai F, Xu H Q and Guo Y 2004 *Phys. Rev. B* **70** 085308

[17] Chen X, Li C F and Ban Y 2008 *Phys. Rev. B* **77** 073307

[18] Chen S Y, Yang S P, Tang Q and Zhou Y L 2017 *J. Comput. Electron.* **16** 347

[19] Liu N Q, Huang L J, Wang R Q and Hu L B 2016 *Chin. Phys. B* **25** 027201

[20] Zhang M H, Wang X F, Song F Q and Zhang R 2018 *Chin. Phys. B* **27** 097307

[21] Gilbert M J and Bird J P 2000 *Appl. Phys. Lett.* **77** 1050

[22] Koga T, Nitta J, Datta S and Takayanagi H 2002 *Phys. Rev. Lett.* **88** 126601

[23] Feng X Y, Jiang J H and Wang M Q 2007 *Appl. Phys. Lett.* **90** 142503

[24] Yokoyama T and Eto M 2009 *Phys. Rev. B* **80** 125311

[25] Puttisong Y, Wang X J, Buyanova I A, Carrere H, Zhao F, Balocchi A, Marie X, Tu C W and Chen W M 2010 *Appl. Phys. Lett.* **96** 052104

[26] Zhang X D 2006 *Appl. Phys. Lett.* **88** 052114

[27] Khodas M, Shekhter A and Finkel'stein A M 2004 *Phys. Rev. Lett.* **92** 086602

[28] Ramaglia V M, Bercioux D, Cataudella V, Filippis G D and Perroni C A 2004 *J. Phys.: Condens. Matter* **16** 9143

[29] Dragoman D 2005 *Physica B* **367** 92

[30] Linder J, Yokoyama T and Sudbø A 2010 *Phys. Rev. B* **81** 075312

[31] Zhai F, Guo Y and Gu B L 2002 *Eur. Phys. J. B* **29** 147

[32] Xu H Z, Liu P J and Zhang Y F 2003 *Phys. Status Solidi B* **240** 169

[33] Hauge E H and Stϕvneng J A 1989 *Rev. Mod. Phys.* **61** 917

[34] Winful H G 2003 *Phys. Rev. Lett.* **91** 260401

[35] Wang L and Guo Y 2006 *Phys. Rev. B* **73** 205311

[36] Lu M W, Chen S Y, Cao X L and Huang X H 2020 *Res. Phys.* **19** 103375

[37] Lu M W, Chen S Y, Cao X L and Wang X H 2021 *IEEE Trans. Electron. Dev.* **68** 860

[38] Guo Q M, Lu M W, Wang X H, Yang S Q and Qin Y J 2021 *Vacuum* **186** 110059

[39] Slobodskyy A, Gould C, Slobodskyy T, Becker C R, Schmidt G and Molenkamp L W 2003 *Phys. Rev. Lett.* **90** 246601